159–202.

[19]C. K. N. Patel and E. D. Shaw (unpublished).

[20]R. J. Collins and J. A. Giordmaine, in *Quantum Electronics*, edited by P. Grivet and N. Bloembergen (Columbia U. P., New York, 1964), Vol. III, pp. 1239–1246.

[21]C. H. Townes, in *Advances in Quantum Electronics*, edited by J. R. Singer (Columbia U. P., New York, 1961), p. 3; see also, W. R. Bennett, Jr., Appl. Opt. Suppl. 1, 24 (1962).

[22]For a review of CO_2 lasers and the transitions seen in laser oscillation see C. K. N. Patel, J. Chim. Phys. 64, 87 (1967). See also, C. K. N. Patel, in *Advances in Lasers*, edited by A. K. Levine (M. Dekker, New York, 1968), Vol. II, p. 1.

[23]M. Born and E. Wolf, *Principles of Optics*, 2nd ed. (Pergamon, New York, 1959).

[24]E. D. Hinkley and T. C. Harman, Appl. Phys. Letters 13, 49 (1968); see also E. D. Hinkley, *ibid.* 16, 351 (1970).

[25]L. M. Roth and P. N. Argyres, in *Physics of III-V Compounds*, edited by R. K. Willardson and A. C. Beer (Academic, New York, 1966), Vol. I, pp. 159–202.

[26]V. P. Makarov, Zh. Eksperim. i Teor. Fiz. Pis'ma v Redaktsiyu 55, 704 (1968) [Soviet Phys. JETP Letters 28, 366 (1969)]; B. S. Wherrett and P. G. Harper, Phys. Rev. 183, 692 (1969).

[27]The InSb samples had the following characteristics (77 °K): (a) $n_e = 1.1\times10^{15}$ cm^{-3}, $\mu = 3\times10^5$ cm^2/V sec; (b) $n_e = 4.7\times10^5$ cm^{-3}, $\mu = 2\times10^5$ cm^2/V sec; (c) $n_e = 1.3\times10^{16}$ cm^{-3}, $\mu = 2.4\times10^5$ cm^2/V sec; (d) $n_e = 2\times10^{16}$ cm^{-3}, $\mu = 1\times10^5$ cm^2/V sec; (e) $n_e = 3\times10^{16}$ cm^{-3}, $\mu = 1\times10^5$ cm^2/V sec; (f) $n_e = 4\times10^{16}$ cm^{-3}, $\mu = 1\times10^5$ cm^2/V sec; and (g) $n_e = 6\times10^{16}$ cm^{-3}, $\mu = 7\times10^4$ cm^2/V sec.

[28]*Tables of Wave Numbers for the Calibration of Infrared Spectrometers* (Butterworths, London, 1961), p. 671.

[29]J. S. Garing, H. H. Nielsen, and K. N. Rao, J. Mol. Spectry. 3, 496 (1959).

[30]H. M. Mould, W. C. Price, and G. R. Wilkinson, Spectrochim. Acta 13, 313 (1959).

[31]C. K. N. Patel, E. D. Shaw, and R. J. Kerl, Phys. Rev. Letters, 25, 8 (1970).

[32]C. K. N. Patel and R. E. Slusher, Phys. Rev. Letters 22, 282 (1969).

PHYSICAL REVIEW B VOLUME 3, NUMBER 4 15 FEBRUARY 1971

Plasmon-Phonon Interference in CdS†

J. F. Scott* and T. C. Damen

Bell Telephone Laboratories, Holmdel, New Jersey 07733

and

J. Ruvalds and A. Zawadowski‡

Department of Physics, University of Virginia, Charlottesville, Virginia 22901

(Received 18 September 1970)

The Raman spectra of plasmons in In- and Ga-doped cadmium sulfide are shown to consist of very asymmetric peaks. A prominent interference shape is exhibited which is very similar to that manifested by anharmonic phonon interactions between two optical phonons, as in $AlPO_4$ and $BaTiO_3$. In the present case, the interaction between the heavily damped plasmon mode and one longitudinal optical phonon is due to the Coulomb interaction. The interference features of the Raman spectrum are related to the electronic (plasmon) and ionic (phonon) charge-density correlation functions, where the ionic charge is multiplied by a factor to include the nonionic (electronic) part of the light-phonon scattering amplitude. In other words, we treat the spectrum as due to interfering amplitudes for scattering into the plasmon state $\langle PL|$ via two channels: one direct, $\langle PL|\alpha|0\rangle$; and one via an intermediate LO-phonon state coupled by the Coulomb interaction, $\langle PL|\text{Coul.}|LO\rangle \times \langle LO|\alpha|0\rangle$. This calculation gives very good agreement with the observed line shape, and demonstrates the inadequacy of treating the spectrum in terms of the usual dielectric function. In the special case when the light-phonon scattering is purely ionic, however, our Green's-function calculation is shown to be equivalent to the dielectric-function formulation which includes both the plasmon and phonon contributions. A detailed comparison of our theory with the experimental spectrum yields an estimate of the relative contributions to the light-phonon scattering amplitude from electronic and ionic charges. For CdS, these contributions are found to be of the same order of magnitude, but opposite in sign.

I. INTRODUCTION AND EXPERIMENTAL

Very recent experiments[1] on inelastic light scattering from plasmons in CdS revealed several anomalies: First, the plasmon line shape was somewhat asymmetric; second, the plasmon linewidth was 25% narrower than calculated from measured Hall mobilities; third, relatively featureless scattering in the 0–200-cm^{-1} region assigned as noncollective electron transitions[2] ("single-particle scattering") occurred for both trace and off-diagonal polarizabilities, whereas the trace scattering is ex-

pected to be completely screened out in the high-charge-density samples examined.[3] In the present paper we present additional experimental data which unambiguously establish the mixture of electronic and ionic origins of all the scattering features in question, together with a many-body random-phase-approximation (RPA) calculation of the line shape, which is in remarkable agreement with our observations. The resulting interpretation of the electron spectrum reconciles the previously reported selection rules[1] and the spin-density fluctuation theory[3] of Hamilton and McWhorter for noncollective electron scattering.

We have been prompted in this work by the strong resemblance between CdS plasmon line shapes and the phonon spectra of $BaTiO_3$[4,5] and $AlPO_4$.[6,7] In the above cases, two different optical phonons contribute to the first-order Raman spectra, and interact via coupling to a two-acoustic-phonon intermediate state.[5-7] A Fano-type[8] interference appears in the spectrum as a result of the anharmonic interactions, in a manner similar to the previous results of Barker and Hopfield,[9] which were based on a classical model.

In CdS, the two excitation modes which contribute directly to the charge-charge correlations are a plasmon and one longitudinal optical phonon. We introduce an "effective" charge to take into account that part (electronic) of the light-*phonon* scattering amplitude which is not due to the charge density induced by the longitudinal phonon (the ionic part). The light-scattering cross section is given by the "effective" charge-charge density correlation function. We have supposed that the interaction between the two modes is purely Coulombic. The interference in the spectrum occurs in the off-diagonal (i.e., plasmon-phonon) terms of the correlation function which includes electronic and ionic charges.

The data were obtained with approximately 200 mW at 5145 Å from an argon ion laser (spectra were checked with 5682-Å Kr II excitation also), and detected by means of a cooled S-20 phototube, a double spectrometer, and electron counting. The spectra were displayed on a strip-chart recorder; typical data are shown in Fig. 1. L_+ and L_- are the upper and lower branches of the coupled LO-phonon and plasmon system.

The samples employed were of several varieties. In-doped CdS from both Harshaw and Eagle Picher were used, with carrier concentrations ranging from 5×10^{17} to 4×10^{19} cm^{-3}. In order to verify the electronic origin of several of the spectral features, we examined *compensated* indium-doped samples with 10^{19} indium ions per cm^3 (in which the features were absent) and also gallium-doped CdS ($n\sim10^{19}$ cm^{-3}) in which they were present. This unquestionably establishes the nature of the scattering peak at ~ 230 cm^{-1} and the "continuum" from 0–200 cm^{-1} as electronic and independent of the dopant.

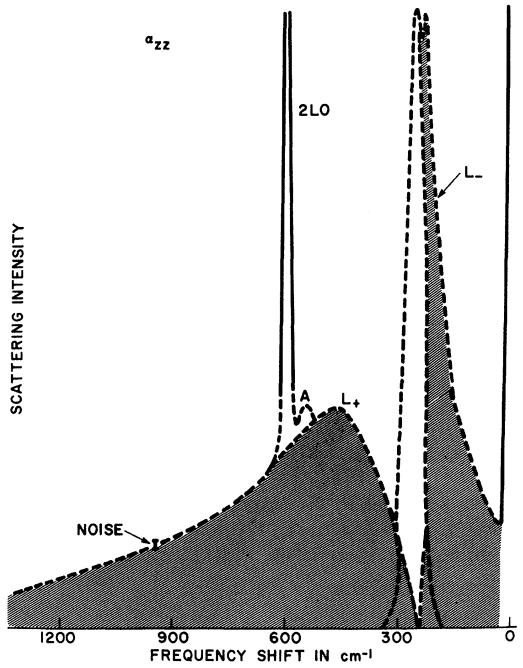

FIG. 1. Observed α_{zz} spectrum of In-doped CdS having $n\approx4\times10^{18}$ cm^{-3}. Spectra were recorded ~ 10 °K with 5145-Å excitation and the geometry $x(zz)y$, with z the [0001] optic axis. The feature labeled "2LO" is a resonant 2 LO$^\Gamma$ excitation; "A" is an ordinary (nonresonant) two-phonon state; L_- is the lower branch of the usual LO-phonon-plasmon pair and is essentially a TO phonon in this highly screened sample. The feature at $\omega\sim280$ cm^{-1} is thought to be bare LO-phonon scattering via bound exciton intermediate states. The shaded portion represents the contribution from the coupled plasmon-phonon system.

We show in Sec. II that the entire complex spectrum shown in Fig. 1 is due to plasmon-phonon scattering. The antiresonant interference shape and the dip at $\omega\approx300$ cm^{-1} are explained in terms of Coulomb coupling between the plasmon and longitudinal phonon. In contrast to Ref. 1, therefore, we interpret the α_{zz} spectrum of n-CdS as devoid of single-particle scattering; this is in accord with the predictions of Ref. 3 which indicate that trace scattering (which arises from charge-density fluctuations) should be vanishingly small for degenerate semiconductors. We believe that the Hamilton-McWhorter theory is appropriate for CdS, despite the hexagonal symmetry, since spin-flip scattering from conduction electrons in CdS has been found to obey cubic selection rules with no anisotropy.[10] The α_{xy} and α_{xz} single-particle spectra in these CdS samples, in accord with expectations, were broad and relatively featureless, extending from 0–600 cm^{-1}, with a full width at half-height of about 200 cm^{-1}, a broad maximum at about 250 cm^{-1}, and

no sharply defined high-energy cutoff (because of the low mobility). The α_{zz} spectrum in Fig. 1 also contains a broad peak at about 275–300 cm^{-1}. We believe that this is because of the bare LO phonon. In undoped CdS, the A_1 LO phonon is at about 298 cm^{-1}. We believe that the LO in Fig. 1 arises from LO phonons having $q \approx 3\times10^6$ cm^{-1}; this scattering occurs via bound exciton intermediate states. These $q \approx 3\times10^6$ cm^{-1} do not couple to plasmons[1] because the latter are damped out (Landau damping) at such momentum values.

II. THEORY OF PLASMON-PHONON INTERFERENCE

Although plasmon-phonon coupling has been extensively studied[11] and considered to be well understood in the case that the two excitations are well separated in energy, the peculiar Raman line shapes discussed in the present work exhibit an overlap and mixing of plasmon and phonon excitations which appear to be rather anomalous. The fact that the plasmon-phonon coupling could give rise to such anomalous structure in the Raman spectrum was not realized in previous theoretical work based on the dielectric-function formulation.

The aims of the present theory are twofold: (a) to explain the experimental anomalies in CdS in terms of plasmon-phonon interference induced by Coulomb coupling, and relate the spectrum to the similar case of the Raman spectrum of two optical phonons interacting via anharmonic coupling to a two-acoustic-phonon continuum,[6,7] and (b) to generalize the theory of light scattering from phonons to include both the phonon-induced charge density (ionic part of the scattering) as well as the nonionic charge density induced by the atomic displacements.[12] The present analysis closely parallels the dielectric-function formulation, which can be obtained from our theory in the special case of purely ionic light-phonon scattering.

Considering the light to be scattered from the charge distribution in the solid, the cross section for Raman scattering is given by the Van Hove formula

$$\frac{d^2\sigma}{d\Omega\, d\omega} \sim \frac{e^2}{\epsilon_\infty^2}\int e^{i\omega t}\langle \rho_q^{\mathrm{eff}}(t)\,\rho_{-q}^{\mathrm{eff}}(0)\rangle\, dt\ , \tag{1}$$

where $d^2\sigma/d\Omega\, d\omega$ denotes the double-differential cross section which is related to the Fourier transform of the effective charge-charge correlation function $e^2\langle \rho_q^{\mathrm{eff}}(t)\,\rho_{-q}^{\mathrm{eff}}(0)\rangle$, where the complex effective charge ρ^{eff} will be explained below. Momentum and energy transfers are denoted by q and ω, respectively. Furthermore, the Fourier transform of the charge distribution $\rho(r)$ is defined as

$$\rho_q = \int e^{-iqr}\rho(r)\, d^3r\ . \tag{2}$$

A "background" dielectric constant ϵ_∞ is defined in our model system as follows: The charge ρ_q to be considered consists of two contributions

$$\rho_q = \rho^e + \rho^i\ , \tag{3}$$

where ρ^e represents the charge of the degenerate electron gas in the conduction band, while ρ^i is associated with the ionic charge induced by phonons. Then ϵ_∞ is the momentum- and energy-independent dielectric constant describing the background charge which is responsible for screening the charge distribution ρ_q by a factor ϵ_∞^{-1}, as can be seen in Eq. (1).

As we have mentioned above, the light-phonon scattering amplitude consists of two parts: an ionic part designated by ρ_q^i and a nonionic part $\rho_q^{(e)\mathrm{phonon}}$. We introduce an "effective" charge $\rho_q^{(i)\mathrm{eff}}$ which describes the *total* phonon contribution to the light-scattering amplitude. Hence, the effective charge for the plasmon-phonon system becomes

$$\rho_q^{\mathrm{eff}} = \rho_q^e + \rho_q^{(i)\mathrm{eff}} = \rho_q^e + \lambda_q\,\rho_q^i\ , \tag{3'}$$

where ρ_q^e is the usual electronic contribution from the plasmons. The coefficient λ_q determines the ratio of electronic to ionic contributions from the *phonon* scattering, i.e.,

$$\lambda_q = (\rho_q^{(e)\mathrm{phonon}} + \rho_q^i)/\rho_q^i\ .$$

The λ_q factor may be complex, and consequently we define $\lambda_q = \lambda' + i\lambda''$ in terms of the real quantities λ' and λ''. If the matrix elements relating the charge density to the phonon mode are considered to be real, then the "effective" charge will in general be complex, since the nonionic contribution of the light-scattering may be proportional to the divergence of atomic displacements (div u) as well as to the displacements u. Consequently we treat λ' and λ'' as adjustable parameters and estimate their relative strengths from a fit of the theoretical line shape to the experimental results shown in Fig. 1.

To calculate the charge-charge correlation function we employ zero-temperature Green's-function techniques.[13] Thus, we introduce the Green's function

$$F(q,t) = i\langle T\,[\rho_q^{\mathrm{eff}}(t)\,\rho_{-q}^{\mathrm{eff}}(0)]\rangle\ , \tag{4}$$

where T denotes the usual time-ordering operator. The corresponding Fourier transform is

$$F(q,\omega) = \int e^{i\omega t}F(q,t)\, dt\ . \tag{5}$$

Following standard procedures,[11] the light-scattering cross section can be related to the imaginary part of $F(q,\omega)$, i.e.,

$$\frac{d^2\sigma}{d\Omega\, d\omega} \sim \frac{e^2}{\epsilon_\infty^2}\ \mathrm{Im}F(q,\omega)\ . \tag{6}$$

The Green's function $F(q, \omega)$ describes the correlation of different kinds of charges, and can be decomposed into three additive contributions of the general form

$$F^{\alpha\beta}(q, t) = i\langle T[\rho_q^\alpha(t)\rho_{-q}^\beta(0)]\rangle \ , \tag{7}$$

where $\alpha = \beta = e$ denotes the purely electronic contribution; $\alpha = \beta = i$ represents the diagonal ionic contribution; and $\alpha = e(i)$, $\beta = i(e)$ corresponds to the mixing of electronic- and ionic-charge distributions. Of these terms [i.e., $F = F^{ee} + 2\lambda' F^{ei} + (\lambda'^2 + \lambda''^2) F^{ii}$], the mixing term F^{ei} is responsible for the plasmon-phonon interference which forms the basis of the present work.

We consider the interaction between the charge distributions to be purely Coulombic and screened by the background. Therefore, in our model, the interaction Hamiltonian can be written as

$$\mathcal{H}_{\text{coulomb}} = \sum_q \frac{2\pi e^2}{q^2 \epsilon_\infty} \rho_q \rho_{-q} \ . \tag{8}$$

In the absence of interactions, only the diagonal terms of the Green's function are nonvanishing and given by

$$F^{\alpha\beta}(q, \omega) \xrightarrow[e^2 \to 0]{} \delta_{\alpha\beta} F^{\alpha(0)}(q, \omega) \ , \tag{9}$$

where $F^{\alpha(0)}$ is the unrenormalized Green's function. With the inclusion of the interaction, these unrenormalized functions

$$F^{(0)} = \sum_{\alpha = e, i} F^{\alpha(0)}$$

determine the dielectric function $\epsilon(q, \omega)$ of electrodynamics according to the well-known expression (for $\omega > 0$),

$$\begin{aligned} \epsilon(q, \omega) &= \epsilon_\infty + (4\pi e^2/q^2) F^{(0)}(q, \omega) \\ &= \epsilon_\infty + (4\pi e^2/q^2)[F^{e(0)}(q, \omega) + F^{i(0)}(q, \omega)] \ . \end{aligned} \tag{10}$$

With regard to the above formula, it should be noted that the dielectric function is usually expressed in terms of the retarded Green's functions. However, in the zero-temperature formalism at positive frequencies, the retarded propagators are identical to the casual Green's functions which are employed throughout the present work.[14]

In order to describe our physical system, we first exhibit the unperturbed Green's functions $F^{e(0)}$ and $F^{i(0)}$:

(i) $F^{e(0)}$ represents the electronic-charge correlation of a conduction-electron band with a degenerate electron gas. The band is assumed to be parabolic with effective mass m^* and the density of electrons is denoted by n. The electron lifetime τ_e due to collision broadening is included as a phenomenological parameter. We are interested in the formation of a plasmon excitation with frequency $\omega_p = (4\pi n e^2/m^* \epsilon_\infty)^{1/2}$, and lifetime $\tau_p = \frac{1}{2}\tau_e$. In the frequency region near the plasmon energy, the well-known expression for the unperturbed Green's function is

$$F^{e(0)}(q, \omega) = -\epsilon_\infty \omega_p^2 q^2 / [4\pi e^2 \omega(\omega + i/\tau_p)]. \tag{11}$$

Neglecting phonon contributions, the dielectric function $\epsilon(q, \omega)$ of the system is obtained by inserting Eq. (11) into (10). This straighforward substitution shows that the real part of $\epsilon(q, \omega)$ tends to zero at $\omega = \omega_p$ as expected.

(ii) $F^{i(0)}$ includes the ionic-charge correlations which are induced by the longitudinal phonons. Since the induced charge is related to the ionic displacement u by the relation $\rho^i \sim \text{div}\, u$ (equivalently $\rho_q \sim iqu_q$, where u_q is the component of the displacement along q_n), the ionic-charge correlation function is proportional to the ionic-displacement Green's function (for $\omega > 0$)

$$\begin{aligned} F^{i(0)}(q, t) &\sim iq^2\langle T[u_q(t)u_{-q}(0)]\rangle \\ &\sim -q^2 \frac{\omega_0^2}{\omega^2 - \omega_0^2 + i\delta} \ , \end{aligned} \tag{12}$$

in the more familiar form.[13] The unperturbed longitudinal phonon frequency is ω_0, which, for $q \sim 0$, is close to the TO-phonon frequency. To relate Eq. (12) to the charge correlation we need to include a positive proportionality factor $(\epsilon_0 - \epsilon_\infty)/4\pi e^2$ which describes the strength of the ionic character of the phonon mode. Then, we obtain[15]

$$F^{i(0)}(q, \omega) = -q^2 \frac{\epsilon_0 - \epsilon_\infty}{4\pi e^2} \frac{\omega_0^2}{\omega^2 - \omega_0^2 + i\delta} \ . \tag{13}$$

In analogy with case (i), we combine Eqs. (13) and (10) to get the dielectric function for the ionic system. In the latter case, the real part of the dielectric function vanishes at a frequency $\omega_l = \omega_0(\epsilon_0/\epsilon_\infty)^{1/2}$, which is the longitudinal phonon frequency renormalized by the polarization of the background charge.

To calculate the Raman-scattering cross section given by Eq. (6), we need to calculate the composite Green's function $F(q, \omega)$ including the Coulomb interaction. However, in order to obtain insight into the physical origin of the plasmon-phonon interference, we consider the different contributions F^{ee}, F^{ii}, and F^{ei} individually. We evaluate the functions $F^{\alpha\beta}$ in the RPA approximation which is illustrated diagrammatically in Fig. 2. In Fig. 2, the plasmon excitations are represented by solid bubbles (corresponding to electron-hole pairs), the wavy lines represent unrenormalized phonons, and the Coulomb interaction is denoted by dotted lines. The Coulomb interaction mixes phonon and plasmon excitations, as can be readily seen from

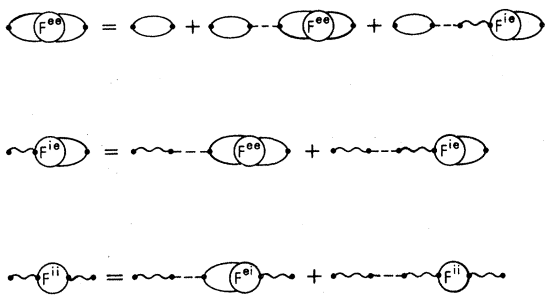

FIG. 2. Diagrammatic representation of the Dyson equations for the charge-charge correlation functions. Solid bubbles denote plasmon (electron-hole) excitations, wavy lines designate phonons, and the dotted lines represent the Coulomb interaction.

the diagrams. The standard technique for summation of the perturbation expansion (a geometric series in the present case) gives

$$F^{\alpha\beta}(q,\omega)=\delta_{\alpha\beta}F^{\alpha(0)}(q,\omega)-\frac{4\pi e^2}{q^2\epsilon_\infty}\times\frac{F^{\alpha(0)}(q,\omega)F^{\beta(0)}(q,\omega)}{1+(4\pi e^2/q^2\epsilon_\infty)[F^{e(0)}(q,\omega)+F^{i(0)}(q,\omega)]}\,, \tag{14}$$

where $\delta_{\alpha\beta}$ is the Kronecker δ and the other quantities appearing in Eq. (14) have been previously defined. Finally, combining Eq. (14) with the expression for the light-scattering cross section [Eq. (6)], we obtain the Raman cross section, including both electronic- (plasmon) and ionic- (phonon) charge distributions,

$$\frac{d\sigma}{d\Omega\, d\omega}\sim\frac{1}{\epsilon_\infty^2}\,\mathrm{Im}[F^{ee}+2\lambda' F^{ei}+(\lambda'^2+\lambda''^2)F^{ii}]\,, \tag{15}$$

where we have used the fact that $F^{ei}=F^{ie}$. The above final result can be expressed in terms of the unrenormalized functions $F^{\alpha(0)}(q,\omega)$ by direct substitution of Eq. (14) into (15).

First, we present the contributions to the cross section from the diagonal terms of Eq. (14). The electronic-electronic term is

$$(1/\epsilon_\infty^2)\,\mathrm{Im}F^{ee}=(\epsilon_\infty\omega_p^2\omega/D\tau_p)\,(\omega^2-\omega_l^2)^2, \tag{16a}$$

and the ionic-ionic term is

$$(1/\epsilon_\infty^2)\,\mathrm{Im}F^{ii}=(\epsilon_\infty\omega_p^2\omega/D\tau_p)\,(\omega_l^2-\omega_0^2)^2\,, \tag{16b}$$

where the denominator includes the function

$$D=[\omega^2\omega_l^2-\omega^4-\omega_p^2(\omega_0^2-\omega^2)]^2+(\omega_l^2-\omega^2)^2\,\omega^2/\tau_p^2, \tag{16c}$$

and $\omega_l=\omega_0(\epsilon_0/\epsilon_\infty)^{1/2}$ denotes the longitudinal phonon frequency. The above diagonal contributions must be positive definite!

The contributions of these terms are indicated by dotted lines in Fig. 3, and exhibit two superimposed peaks without interference effects. On the other hand, the cross term F^{ei} gives a negative contribution to the Raman spectrum as can be seen from the analytic expression

$$(1/\epsilon_\infty^2)\,\mathrm{Im}F^{ei}=(\epsilon_\infty\omega_p^2\omega/D\tau_p)\,(\omega_l^2-\omega_0^2)\,(\omega^2-\omega_l^2)\,, \tag{16d}$$

which is shown by dashed lines in Fig. 3. It is interesting to note that the mixing term F^{ei} is negative only for $\omega<\omega_l$, and exhibits an antisymmetric character as shown in Fig. 3. Assuming for the moment that the "effective" charge induced by the phonon is real, i.e., $\lambda''=0$, it is apparent from Fig. 3 that the mixing term F^{ei} gives rise to a deep minimum {in fact, an exact zero at $\omega=[\omega_l^2-\lambda'(\omega_l^2-\omega_0^2)]^{1/2}$} at a frequency between the peaks corresponding to the hybridized plasmon and phonon excitations (L_+ and L_-). Therefore, these mixing terms, which are a consequence of the plasmon-phonon coupling, are responsible for the antiresonance feature in the Raman spectrum shown in Fig. 1. However, it is rather apparent that the total calculated spectrum

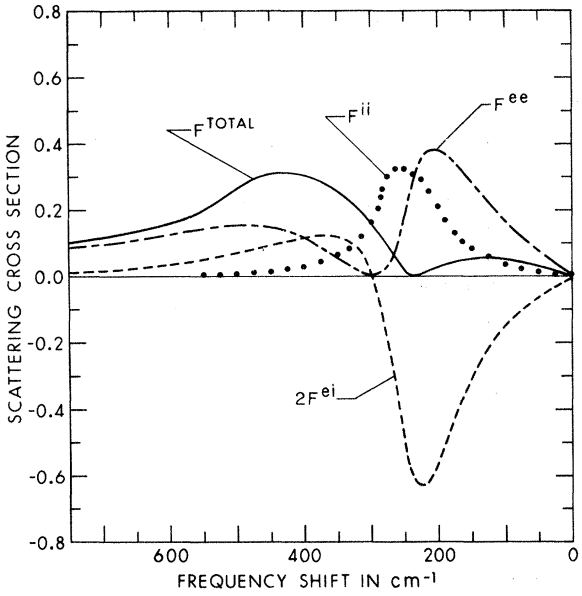

FIG. 3. Calculated spectrum for the coupled plasmon-phonon system in the limiting case of a real "effective" charge ($\lambda'=1$, $\lambda''=0$). Dotted and dot-dashed lines represent diagonal contributions F^{ii} and F^{ee}, respectively, while the dashed line shows the mixing term $2F^{ei}$ which gives rise to the deep dip (antiresonance) in the total spectrum given by the solid line. The parameters used were $\omega_0=230$ cm^{-1}, $\omega_l=300$ cm^{-1}, $\omega_p=500$ cm^{-1}, and plasmon width $\Gamma_p=660$ cm^{-1}. These parameters were taken from the Raman data discussed in the text.

(assuming $\lambda'' = 0$ and $\lambda' = 1$) gives a poor fit to the experimental data for CdS, especially in the low-energy region near the L_- peak. It is important to note that our theoretical results in this limiting case of a real "effective" charge (and taking $\lambda' = 1$) reproduce the light-scattering cross section derived on the basis of a dielectric-function formulation by Varga[16] and others. The correspondence between the dielectric-function formalism and our theory is the following: The Raman cross section can be written as

$$\frac{d\sigma}{d\Omega\, d\omega} \sim \mathrm{Im}\frac{1}{\epsilon(q,\omega)}, \tag{17}$$

where the dielectric function is defined in Eq. (10) as

$$\epsilon(q,\omega) = \epsilon_\infty + (4\pi e^2/q^2)\,[F^{e(0)}(q,\omega) + F^{i(0)}(q,\omega)]. \tag{18}$$

Substituting the values of the unperturbed Green's function $F^{\alpha(0)}$ from Eqs. (11) and (12) into (18), we obtain the dielectric function in the form derived by other authors[16]:

$$\epsilon = \epsilon_\infty + \frac{(\epsilon_0 - \epsilon_\infty)\omega_0^2}{\omega_0^2 - \omega^2} - \frac{\epsilon_\infty \omega_p^2}{\omega^2 + i\omega/\tau_p}\ . \tag{19}$$

Note, however, that this correspondence holds *only* in the special case $\lambda'' = 0$ and $\lambda' = 1$, and the theoretical light-scattering cross section for this limiting case is in disagreement with experiment.

To resolve the above discrepancy between theory and experiment we need to consider the light-scattering cross section including the possibility of a complex "effective" charge as discussed above. Thus, the general expression for the Raman cross section is obtained by inserting Eqs. (16) into (15); our final result can be written in the form

$$\frac{d\sigma}{d\Omega\, d\omega} \sim (\epsilon_\infty \omega_p^2 \omega/D\tau_p)\,\{[\omega^2 - \omega_l^2 + \lambda'(\omega_l^2 - \omega_0^2)]^2 + \lambda''(\omega_l^2 - \omega_0^2)^2\}\ . \tag{20}$$

The theoretical scattering cross section given by Eq. (20) is shown by the curves in Fig. 4. The calculation was made using the following parameters: $\epsilon_\infty = 5.2$ from Ref. 17; $\epsilon_0 = (\omega_{LO}/\omega_{TO})^2$, with $\omega_{LO} = 300\,\mathrm{cm}^{-1}$ and $\omega_{TO} = 230\,\mathrm{cm}^{-1}$ from Raman measurements of the A_1 phonons; plasmon energy $\omega_p = 500\,\mathrm{cm}^{-1}$ and width $\Gamma_p = 660\,\mathrm{cm}^{-1}$ from the data shown in Fig. 1. The values taken for the plasmon parameters ω_p and Γ_p are compatible with Hall measurements of carrier concentration and mobility for the sample. In Fig. 4, the solid curve describes the calculated spectrum for a *real* effective charge using parameters $\lambda' = 0.2$ and $\lambda'' = 0.0$, which were chosen to fit data of Fig. 1. Note that a value of $\lambda' = 0.2$ moves the "dip" closer to the LO-phonon frequency ($\omega_{LO} = 300\,\mathrm{cm}^{-1}$) and accentuates the L_- peak near $200\,\mathrm{cm}^{-1}$. The solid line bears a remarkable resemblance to the experimental data of Fig. 1, in contrast to the results of the dielectric-function formulation shown in Fig. 3. To demonstrate the effect of a "complex" charge on the spectrum, we plot the theoretical cross section with dotted lines in Fig. 4 using parameters $\lambda' = 0.2$ and $\lambda'' = 0.5$: It is apparent that the complex charge enhances the L_- somewhat. However, in the case of CdS, the choice of a purely real charge to calculate the spectrum seems adequate in fitting experiment.

One feature of the experimental data which remains puzzling is the existence of the double-peak structure near $\omega \sim 230$–$280\ \mathrm{cm}^{-1}$. Since the latter structure appears in the Raman spectrum of CdS with quite different dopant concentrations, [1] it is reasonable to consider the structure as intrinsic to CdS. We believe the double-peak structure consists of two contributions: (a) a contribution from the TO-phonon mode with A_1 symmetry at $\omega_{TO} \simeq 228\ \mathrm{cm}^{-1}$, [18] which is Raman active for the α_{zz} spec-

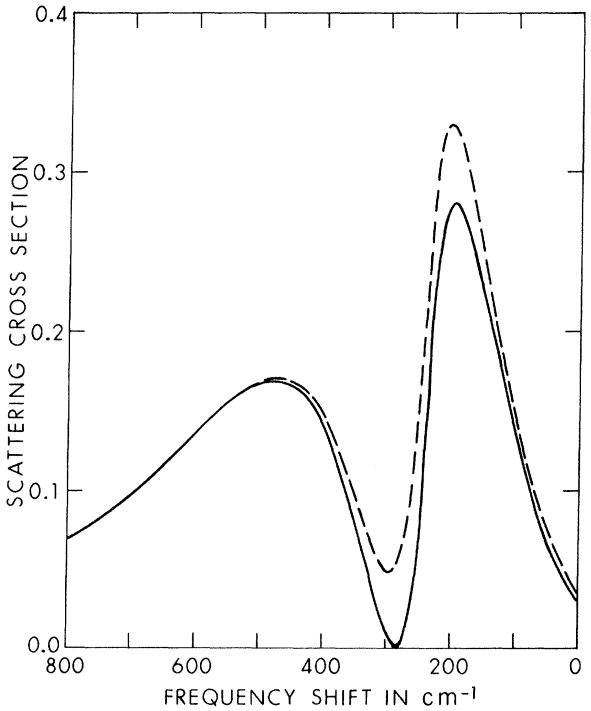

FIG. 4. Calculated spectrum for the plasmon-phonon system using the same parameters as in Fig. 3, but including different values for the "effective" charge parameters. The solid line represents a *real* charge with $\lambda' = 0.2$, $\lambda'' = 0$; while the dotted line exhibits the spectrum for a complex charge ($\lambda' = 0.2$ and $\lambda'' = 0.5$), respectively.

trum, and (b) allowed α_{zz} LO-phonon scattering near 280 cm^{-1} due to $q \approx 3\times10^6$ cm^{-1} LO phonons for which Raman scattering via bound exciton intermediate states is possible. In the interest of clarity we have not attempted to include the latter two contributions in the theoretical cross section. Addition of these phonon contributions would certainly improve agreement with experiment, but necessitates introduction of additional parameters.

It is amusing to realize the basic similarity between the plasmon-phonon interference and the indirect coupling of two optical phonons mediated by the acoustic-phonon continuum.[7] A common feature of both problems is the existence of two excitations which are sufficiently broad in energy so that their spectra overlap. Interactions between the excitations cause a mixing of the two excitation modes. In either case, light is directly coupled to both excitations which can be described as a linear combination of two operators: (i) "effective" charge distribution operators ($\rho = \rho^e + \lambda_q \rho^i$) in the plasmon-phonon case; and (ii) a linear combination of phonon field operators in the phonon-phonon case discussed in Ref. 7. We have seen that the light-scattering cross section is related to a correlation function whose diagonal terms mainly determine the structure of two superimposed peaks, while the cross terms of the correlation function cause the deep interference minimum (antiresonance). The mathematical similarity between the present results and those of Ref. 7 is quite apparent in the limiting case $\lambda' = 1$, $\lambda'' = 0$; as can be seen by replacing the phonon Green's functions $D_\alpha^{(0)}$ in Ref. 7 by the charge-correlation Green's functions $F^{\alpha(0)}$ and simultaneously making the replacement

$$g_\alpha g_\beta D_2^{(0)ac} \rightarrow -4\pi e^2/q^2\epsilon_\infty ,$$

where g_α is the anharmonic interaction constant which couples the optical phonons to a two-acoustic-phonon continuum described by the two-phonon Green's function $D_2^{(0)ac}$. There is an important difference between the two cases, however. In the case of two optical phonons, the lifetime of an optical phonon was mainly determined by decay to two acoustic phonons, which are also responsible for the indirect coupling between the optical phonons. In the present case, the plasmon mode has a broad width due to single-electron (or hole) collision broadening. In the latter case, the unrenormalized, phonon width is negligible in comparison to the plasmon width. Nevertheless, the plasmon-phonon spectrum tends to zero at $\omega = \omega_0$, in a manner quite similar to the two-optical-phonon spectrum of $AlPO_4$.[6,7] The fact that the experimental spectrum for CdS does not dip completely to zero near $\omega \sim 280$ cm^{-1} could be a consequence of a complex "effective" charge as seen in Fig. 4, but more likely is due to the scattering from the LO phonon discussed above.

In conclusion it is worth mentioning that the present theory can be generalized to include a direct electron-phonon interaction which may contribute to the LO-phonon–plasmon coupling.

III. SUMMARY

We have presented the first plasmon data in which linewidths are much greater than the $\omega(L_+) - \omega(\mathrm{LO})$ separation, together with an analysis which accurately describes line shapes under these conditions. The analysis is in no sense dependent upon any parameters particular to CdS; hence the phenomenon should be present in all heavily doped semiconductors in which low mobility causes plasmon linewidths to be greater than $(\omega_{LO} - \omega_{TO})$. On the basis of the RPA approximation, a Green's-function calculation, which makes the physical origin of the interference slopes explicit, has been given. The present analysis reconciles previously reported anomalies in the CdS plasmon spectrum.[1] The low-frequency α_{zz} scattering is shown to be part of the L_- branch and not single-electron scattering; the mobility determined linewidth is shown not to characterize L_+, but yields a full width at half-height for the combined L_+/L_- spectrum; finally, the distinct asymmetries of L_+ and L_- are completely explained.

A comparison between the experimental Raman spectrum and our theory has shown that the ionic and electronic parts of the light-*phonon* scattering are of the same order of magnitude. It is interesting to note that the latter two contributions have opposite signs, as demonstrated by the value $\lambda' = 0.2$ (i.e., $\lambda' < 1$) which was obtained from fitting the theory to experiment. Furthermore, it appears that the imaginary part λ'' of the effective charge should be relatively small. The determination of the relative signs of electronic and ionic parts of the phonon contribution to the phonon amplitude was possible due to the coexistence of the plasmon peak. The plasmon spectrum is well understood in terms of the simple electromagnetic coupling to light. In the absence of plasmon contributions, the phonon cross section is proportional to $|\lambda_q|^2$. Hence, a much more accurate estimate of the ionic (electronic) part of the phonon scattering could be obtained from samples with varying dopant concentrations, especially in the case when the plasmon and phonon peaks are well separated in energy. One example of the latter situation is GaAs,[19] where a large discrepancy exists between the observed plasmon-phonon intensities and the value predicted by theories based on the dielectric-function formalism.[20]

Note added in proof. The contributions termed "electronic" and "ionic" scattering in the present paper are more commonly designated in the litera-

ture as "deformation-potential" and "electro-optic" contributions, respectively. The relative magnitudes of the "deformation-potential" and "electro-optic" contributions have been found to be comparable and opposite in sign for a number of compounds.[21–23] Comparable contributions of the same sign have been estimated for Zno,[24] however.

ACKNOWLEDGMENTS

We are indebted to Professor P. A. Wolff and Professor R. Loudon for very valuable and stimulating discussions. One of us (A. Z.) has greatly benefited from discussions with Professor E. Burstein.

---

†Research supported in part by the Center for Advanced Studies at the University of Virginia.

*Present address (until September 1971): Department of Natural Philosophy, The University of Edinburgh, Edinburgh, Scotland.

‡Permanent address: Central Research Institute for Physics, Budapest, Hungary.

[1]J. F. Scott, T. C. Damen, R. C. C. Leite, and Jagdeep Shah, Phys. Rev. B 1, (1970).

[2]A. Mooradian, Phys. Rev. Letters 20, 1102 (1968); David Pines, *Elementary Excitations in Solids* (Benjamin, New York, 1964), pp. 138–156.

[3]D. C. Hamilton and A. L. McWhorter, in *Light Scattering Spectra of Solids*, edited by G. B. Wright (Springer-New York, 1969), pp. 309–316.

[4]D. L. Rousseau and S. P. S. Porto, Phys. Rev. Letters 20, 1354 (1968).

[5]A. Pinczuk, E. Burstein and S. Ushioda, Solid State Commun. 7, 139 (1969).

[6]J. F. Scott, Phys. Rev. Letters 24, 1107 (1970).

[7]A. Zawadowski and J. Ruvalds, Phys. Rev. Letters 24, 1111 (1970).

[8]U. Fano, Phys. Rev. 124, 1866 (1970).

[9]A. S. Barker and J. J. Hopfield, Phys. Rev. 135, A1732 (1964).

[10]J. F. Scott and P. A. Fleury, in Proceedings of the International Conference on Raman Spectroscopy, Oxford, England, 1970 (unpublished).

[11]P. A. Wolff, in *Light Scattering Spectra of Solids*, edited by G. Wright (Springer, New York, 1969), p. 273, and references cited therein.

[12]M. Born and K. Huang, *Dynamical Theory of Crystal Lattices* (Oxford U. P., London, 1966), p. 206.

[13]A. A. Abrikosov, L. P. Gorkov, and I. E. Dzyaloshinski, *Methods of Quantum Field Theory in Statistical Physics*, edited by R. Silverman (Prentice-Hall, Englewood Cliffs, N. J., 1963).

[14]According to the Kubo formula, the right-hand side of Eq. (10) is the polarization-polarization correlation function which can be transformed to the charge-charge correlation function using the relation $\rho = \mathrm{div}\, P$ (or equivalently, $\rho_q = iqP_q$), where P is the polarization. This transformation introduces the factor q^{-2} in Eq. (10). Note that this factor $(4\pi e^2 q^{-2})$ differs from the Fourier transform of the screened Coulomb interaction by a factor ϵ_∞.

[15]The minus sign in Eqs. (12) and (13) enters as a consequence of the definition of the phonon Green's function with a factor $(-i)$ in the front of the T product (see, for example, Ref. 12).

[16]B. B. Varga, Phys. Rev. 137, A1896 (1965).

[17]T. M. Bieniewski and S. J. Czyak, J. Opt. Soc. Am. 53, 496 (1963).

[18]B. Tell, T. C. Damen, and S. P. S. Porto, Phys. Rev. 144, 771 (1966).

[19]A. Mooradian and A. L. McWhorter, Phys. Rev. Letters 19, 849 (1967).

[20]Unfortunately, the good agreement between theory and experiment claimed in Ref. 19 is based on an erroneous factor of ω^{-4} in the intensity [Eq. (2) in Ref. 19], which is in disagreement with results obtained by other authors (e.g., Ref. 11). The corrected expression for the light-scattering amplitude based on the dielectric-function formalism predicts an L_- peak one order of magnitude smaller then observed experimentally.

[21]W. L. Faust and Charles H. Henry, Phys. Rev. Letters 17, 1265 (1966).

[22]R. C. C. Leite, T. C. Damen, and J. F. Scott, in *Light Scattering Spectra of Solids*, edited by G. Wright (Springer, New York, 1969), p. 359.

[23]S. Ushioda, A. Pinczuk, W. Taylor, and E. Burstein, in Proceedings of the II-VI Semiconducting Compounds 1967 Conference, p. 1185 (unpublished).

[24]S. P. S. Porto, B. Tell, and T. C. Damen, Phys. Rev. Letters 16, 450 (1966).